Materials Transactions, Vol. 61, No. 1 (2020) pp. 213 to 220

Relation of Size Distribution of Cracks in Superconducting Layer to Critical Current Distribution under Small Voltage Probe Spacing in REBCO-Superconducting Composite Tape

Shojiro Ochiai[1,*] and Hiroshi Okuda[2]

[1]*Elements Strategy Initiative for Structural Materials, Kyoto University, Kyoto 606-8501, Japan*
[2]*Department of Materials Science and Engineering, Kyoto University, Kyoto 606-8501, Japan*

The relation of distribution of crack size to that of critical current under small voltage probe spacing in RE(Y, Sm, Dy, Gd, ...)$Ba_2Cu_3O_{7-\delta}$ layer-coated superconducting tape with stress-induced cracks was studied with a Monte-Carlo simulation method in combination with a model of current shunting at cracks. First, it was shown that the experimentally observed feature that the critical current decreases with increase in distribution width of crack size and voltage probe spacing was reproduced by the present simulation. Then it was revealed that (i) the largest crack among all cracks in the region between the voltage probes plays a dominant role in determination of critical current, and, (ii) when the size of the largest crack is fixed, the large difference in crack size among all cracks acts to raise the critical current value and to reduce the *n*-value, and, in this phenomenon, the reduction of *n*-value with increasing difference in crack size is more dominant than the increase of critical current. Finally, it was shown that the distribution of critical current can be described using the Gumbel's extreme value distribution function as a first approximation under small voltage probe spacing where the influence of the difference in crack size on critical current is relatively small.
[doi:10.2320/matertrans.MT-MAW2019001]

(Received May 15, 2019; Accepted October 28, 2019; Published November 29, 2019)

Keywords: *superconducting tape, critical current distribution, crack size distribution, voltage probe spacing, extreme value distribution*

1. Introduction

Superconducting tapes are subjected to thermal, mechanical and electromagnetic stresses/strains in fabrication and operation. When such stresses cause cracking of the superconducting layers/filaments, the critical current (I_c) and *n*-value of RE(Y, Sm, Dy, Gd, ...)$Ba_2Cu_3O_{7-\delta}$ layer-coated tapes (hereafter noted as REBCO tapes)[1–8] and $Bi_2Sr_2Ca_2Cu_3O_{10+x}$(Bi2223)[9–14]-, MgB_2[15]-, Nb_3Al[16]- and Nb_3Sn[17]-filamentary tapes are reduced seriously. As the cracking of the coated layers/filaments is caused heterogeneously, the I_c- and *n*-values are different from position to position within a specimen[6,8–11,16] and also from specimen to specimen.[8,11,13,14] It has been shown that such a phenomenon is dependent on the specimen length/voltage probe spacing (L) under existence of defects not limited to cracks.[5,8,11,14,18,19]

Recently, the authors has been developing a simulation method, based on a Monte Carlo method combined with a current shunting model at cracks, as a tool to study the influences of distribution of crack size and L on I_c- and *n*-values.[20–24] Here, the crack size refers to the crack length, existing perpendicularly to the current transport-direction. With the developed simulation method, the feature "I_c- and *n*-values decrease with increasing distribution width of crack size and with increasing L in heterogeneously cracked superconducting tapes" was reproduced successfully.[20–24] Also it was found that this phenomenon is induced by the increase in size of the largest crack among all cracks in the region between the voltage probes.[22,23] Furthermore, by using the simulation method, the experimentally observed phenomenon "under coexistence of a large defect and multiple small defects, I_c-value is low when the voltage probe spacing is small but it goes up with increasing voltage probe spacing[18]" was reproduced.[24]

For analysis of the distributed I_c- and *n*-values of the region/specimen consisting of multiple cracked sections, the authors have been attempting to calculate the upper and lower bounds of I_c- and *n*-values by using the voltage-current curve of the section with the largest crack among all cracks in the region between the voltage probes.[22–24] The application of the upper and lower bounds approach to the simulation results revealed that, for a given size of the largest crack, the simulation results of I_c- and *n*-values are in between the upper and lower bounds. Also it was confirmed that, in any voltage probe spacing, I_c-value shifts from the lower to upper bound, and, in contrast, *n*-value shifts from the upper to lower bound with increase in distribution width of crack size.[22–24]

As stated above, the simulation method and the upper-lower bounds approach for I_c- and *n*-values are useful to describe the relation of I_c- and *n*-values to the distribution of crack size and voltage probe spacing/specimen length. As a next step, the authors have been trying to describe/predict the distribution of the critical current values from the viewpoint of the distribution of crack size, by extensive application of the simulation method and the upper-lower bounds approach mentioned above to wide variety of voltage probe spacing/specimen length. It was found that the I_c distribution can be described satisfactorily as a first approximation when the voltage probe spacing is small. This result shows that the present approach, based on the distribution of the crack size, provides a useful concept and a useful tool towards the description/prediction of the distribution of critical current values of heterogeneously cracked short specimens/short regions between the voltage probes. The present paper reports the approach and the results.

*Corresponding author, E-mail: shojiro.ochiai.54n@st.kyoto-u.ac.jp

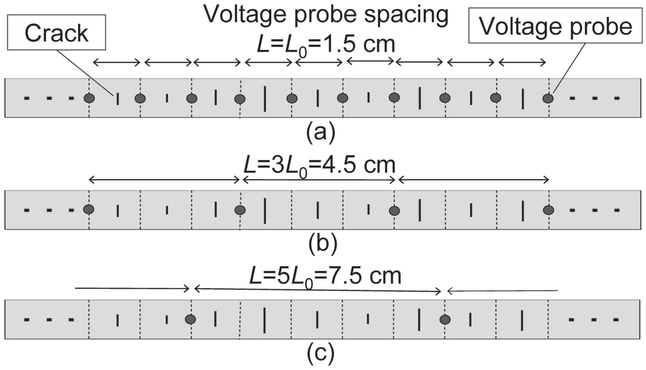

Fig. 1 Schematic representation of the model tape having 120 local sections. Each section with a length L_0 (1.5 cm) has a crack of different size from each other. The voltage probes were attached in a step of $L = L_0$, $3L_0$ and $5L_0$, as shown in (a), (b) and (c), respectively. The regions between the voltage probes consist of 1, 3 and 5 sections.

2. Model Superconducting Tape and Simulation Procedure

2.1 Model tape

The configuration of the model tape and the locations of the voltage probes are shown in Fig. 1. The model tape with a length of 180 cm is constituted of a series of 120 local sections with a length $L_0 = 1.5$ cm. Each local section has one crack with different size from each other. The depth of the crack was taken to be equal to the thickness of the superconducting REBCO layer. The voltage probes were attached to the tape in a step of the distance $L = L_0$ (1.5 cm), $3L_0$ (4.5 cm) and $5L_0$ (7.5 m), as shown in Fig. 1(a), (b) and (c), respectively. Hereafter, the region between the voltage probes is called simply as region. There were 120, 40 and 24 regions in the model tape when $L = 1.5$ cm, 4.5 cm and 7.5 cm, respectively.

2.2 Simulation procedure

A Monte Carlo simulation combined with a model of current shunting at cracks was carried out in a similar manner to our recent works.[20–24] The outline is briefly described below.

2.2.1 Derivation of the voltage (V)-current (I) curves of sections ($L = L_0 = 1.5$ cm)

The voltage (V)–current (I) curves of the sections were derived with the modified form[2,4,6,8,14,20–24] of the crack-induced current shunting model proposed by Fang *et al.*[9] We define the I_c- and n-value of the sections in the non-cracked state as I_{c0} and n_0, respectively; the ratios of cross-sectional area of the cracked part and ligament part to the total cross-sectional area of the REBCO layer, as f and $1 - f$, respectively, where the f and $1 - f$ are the same as the ratios of the crack size and ligament size to the total transverse length of the REBCO layer whose transverse cross-section is rectangular in shape; the current transported by the REBCO layer in the ligament part as I_{RE}; the voltage developed at the ligament part that transports current I_{RE} as V_{RE}; the shunting current at the cracked part as I_s; electric resistance of the shunting circuit as R_t; the voltage developed at the cracked part by shunting current I_s as V_s ($= I_s R_t$) and the current transfer length in the shunting circuit as s ($\ll L_0$). The critical electric field for estimation of I_c is expressed as E_c ($= 1\,\mu$V/cm in this work).

The V–I curve of the cracked section is expressed as,[2,4,20–24)]

$$V = E_c L_0 \left(\frac{I}{I_{c0}}\right)^{n_0} + V_{RE} \tag{1}$$

$$I = I_{RE} + I_s = I_{c0} L_p \left[\frac{V_{RE}}{E_c L_0}\right]^{1/n_0} + \frac{V_{RE}}{R_t} \tag{2}$$

where L_p ($= (1 - f)(L_0/s)^{1/n_0}$) is the ligament parameter of section, which was derived by the authors[2,4,14,20–24] through a modification of the formulations of Fang *et al.*[9] The ligament parameter L_p in eq. (2) was used to monitor the ligament area fraction $1 - f$. It was used also as a monitor of crack size f, since $1 - f$ and f have one to one correspondence; small/large ligament area fraction $1 - f$ corresponds to large/small crack area fraction f and also the standard deviation of the ligament area fraction $1 - f$ is the same as that of the crack area fraction f. Hence, the standard deviation of L_p, ΔL_p, can be used as a monitor of the distribution width of crack size; the larger the ΔL_p-value, the wider is the distribution of crack size.

The distribution of L_p was formulated using the normal distribution function, as in our former works.[20–24] Noting the average of L_p values as $L_{p,ave}$, the cumulative probability $F(L_p)$ and density probability $f(L_p)$ are expressed as follows.

$$F(L_p) = \frac{1}{2}\left\{1 + \mathrm{erf}\left(\frac{L_p - L_{p,ave}}{\sqrt{2}\Delta L_p}\right)\right\} \tag{3}$$

$$f(L_p) = \frac{1}{\sqrt{2\pi}\Delta L_p}\exp\left\{-\frac{(L_p - L_{p,ave})^2}{2(\Delta L_p)^2}\right\} \tag{4}$$

The $L_{p,ave}$ was taken to be 0.67 to pick up a representative situation where the cracks reduce the I_c of sections by $\approx 1/3$ on average from the non-cracked state. To obtain the distribution of I_c under wide variety of distribution of the crack size, five cases of $\Delta L_p = 0.01$, 0.025, 0.05, 0.10 and 0.15 were taken up. The L_p value for each cracked section was given by a Monte Carlo method by generating a random value *RND* in the range of $0\sim1$, setting $F(L_p) = RND$ and substituting the values of $L_{p,ave}$ and ΔL_p in eq. (3).

The V–I curve of each cracked section was calculated by substituting the L_p-value obtained by the Monte Carlo method, and the values of $R_t = 2\,\mu\Omega$, $I_{c0} = 200$ A and $n_0 = 40$ taken from our former experimental work,[6] into eqs. (1) and (2).

2.2.2 Derivation of voltage (V)-current (I) curves of the regions between the voltage probes and criteria for estimation of critical current and n-value

The voltage probe spacing L was given to be 1.5 cm, 4.5 cm and 7.5 cm. For $L = 1.5$ cm, the V–I curves of the sections were obtained by the procedure stated in 2.2.1. As the regions with $L = 4.5$ and 7.5 cm consist of a series electric circuit of the number of N sections (Fig. 1(a)), ($N = 3$ and 5 for $L = 4.5$ and 7.5 cm, respectively), the V–I curves of the regions were synthesized using the V–I curves of the sections by

$$V = \sum_{i=1}^{N} V_{S(i)} \tag{5}$$

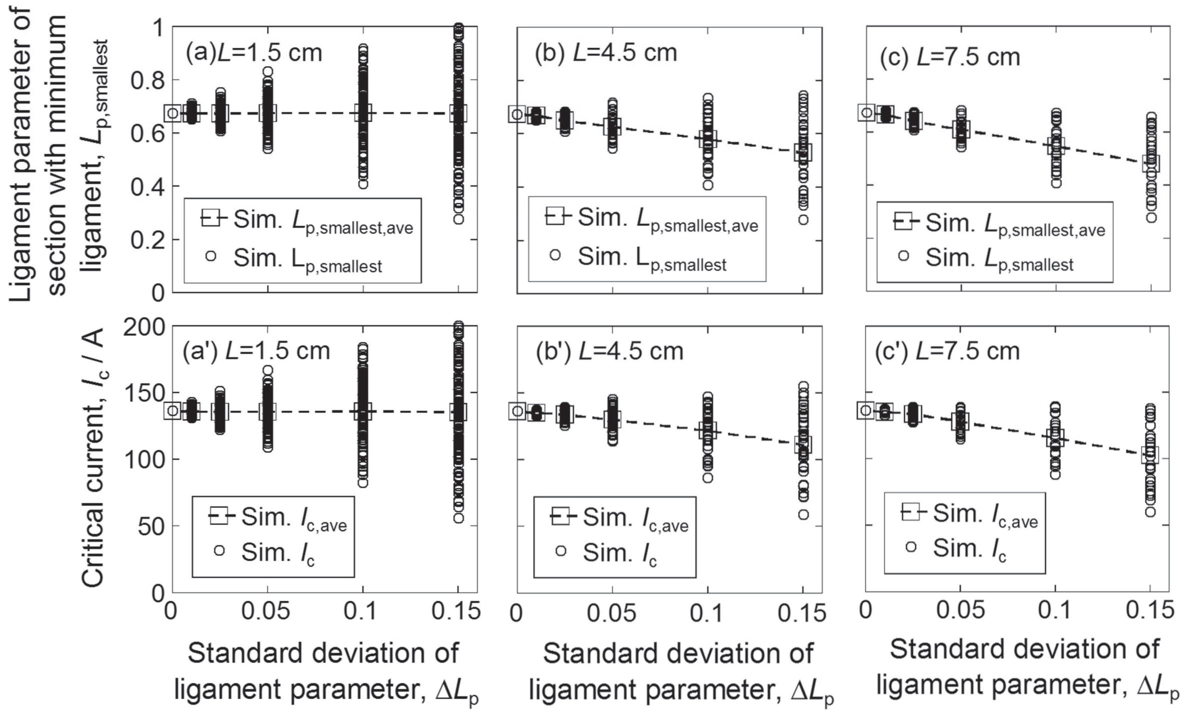

Fig. 2 Simulation results of the values of (a, b, c) the ligament parameter of the smallest ligament (= largest crack)-section $L_{p,smallest}$ and (a′, b′, c′) the critical current I_c, plotted against the standard deviation of the ligament parameter ΔL_p. (a, a′), (b, b′) and (c, c′) show the results for $L = 1.5$ cm, 4.5 cm and 7.5 cm, respectively.

$$I = I_{S(i)} \quad (i = 1 \text{ to } N) \tag{6}$$

where $V_{S(i)}$ and $I_{S(i)}$ are the voltage and current of section i, respectively.

From the calculated V–I curves, the I_c-values for $L = 1.5$, 4.5 and 7.5 cm were obtained by the critical electric field criterion of $E_c = 1\,\mu V/cm$ (corresponding to the critical voltage $V_c = E_c L$). The n-value was obtained by fitting the E–I curve to the form of $E \propto I^n$ in the electric field range of $E = 0.1{\sim}10\,\mu V/cm$, namely by fitting the V–I curve to the form of $V \propto I^n$ in the voltage range of $V = 0.1E_cL \sim 10E_cL\,\mu V$.

3. Results and Discussion

3.1 Simulation results of the distribution of ligament parameter of the smallest ligament (= largest crack)-section, $L_{p,smallest}$, among the sections in the region between the voltage probes and the distribution of the region's I_c

Figure 2 shows the simulation results of the values of (a, b, c) the ligament parameter of the smallest ligament (= largest crack)-section, $L_{p,smallest}$, among the sections existing in the region between the voltage probes and (a′, b′, c′) the region's I_c, plotted against the standard deviation of the ligament parameter ΔL_p which refers to the distribution width of the ligament size, which is equal to the distribution width of crack size, as stated in subsection 2.2.1. (a, a′), (b, b′) and (c, c′) show the results for $L = 1.5$ cm, 4.5 cm and 7.5 cm, respectively.

The following features are read from the results in Fig. 2.

(a) The $L_{p,smallest}$-value, referring to the ligament parameter of the smallest ligament (largest crack)-section, and I_c-values of the regions are different from each other, showing that both of the size of the largest crack and the I_c-value are different from region to region and they vary along the tape length, as has been observed experimentally.[8–11,13,14,16]

(b) The $L_{p,smallest}$-value decreases with increasing distribution width of the ligament parameter (= distribution width of crack size) ΔL_p and voltage probe spacing (= length of the region between the voltage probes) L. Also, similarly to the $L_{p,smallest}$-value, the I_c-value decreases with increasing ΔL_p and L.

(c) Comparing the distributions of $L_{p,smallest}$-values in (a, b, c) with those of I_c-values in (a′, b′, c′), the distributed values of $L_{p,smallest}$ and the average of $L_{p,smallest}$-values, $L_{p,smallest,ave}$, seem to be in a similar relationship to the distributed values of I_c and the average of I_c-values, $I_{c,ave}$. This feature suggests that the size of the smallest ligament (= largest crack) among all cracked sections plays a dominant role in determination of the region's I_c.

3.2 Influence of the smallest ligament (largest crack)-section among all sections in the region between the voltage probes on the region's I_c and n-value

The superconductivity of the region composed of multiple sections is lost first at the section with the largest crack (= with the smallest ligament). The voltage developed at the largest crack-section is highest among all sections and it contributes most significantly to the synthesis of the voltage of the region. Using this phenomenon, the authors have been showing that the upper and lower bounds of I_c and n-value of the region can be calculated with the V–I curve of the section having the largest crack by setting the following two extreme cases A and B.[20–24)

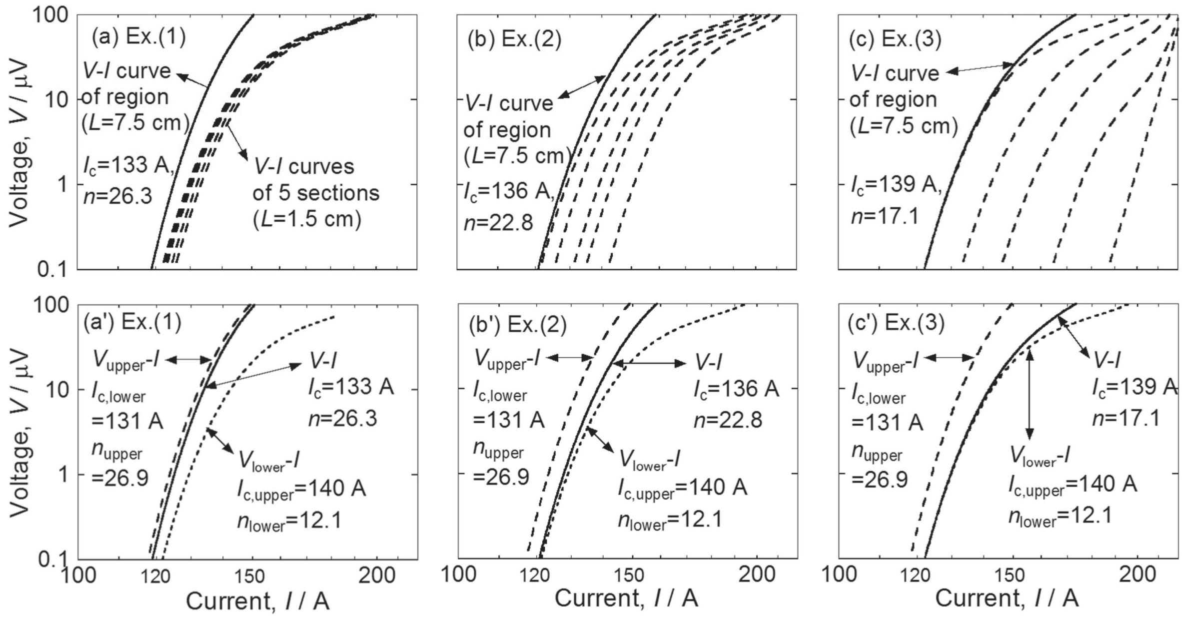

Fig. 3 Examples of (a, b, c) V–I curves of the 7.5 cm-region and the five 1.5 cm-sections that constitute the 7.5 cm-region, and (a′, b′, c′) V–I, V_{upper}–I and V_{lower}–I curves of the 7.5 cm-region, where the V_{upper}–I and V_{lower}–I curves were calculated based on cases A and B using the V–I curve of the largest crack-section. (a, a′), (b, b′) and (c, c′) show the results of Ex.(1), Ex.(2) and Ex.(3), referring to small, intermediate and large difference in crack size among the five sections, respectively. The ligament parameter of the smallest ligament (= largest crack)-section, $L_{p,smallest}$, is common in Ex.(1), Ex.(2) and Ex.(3), while the ligament parameter values of the other four sections are different among the examples.

Case A: an extreme case where the crack size is the same and hence all sections have the largest crack. The voltage of the region, given by the sum of the voltage of all sections existing in the region, corresponds to the upper bound of the voltage of the region, V_{upper}. Therefore, the n-value of the region, defined as the index in the form of $V \propto I^n$, corresponds to the upper bound, n_{upper}. On the contrary, as the increase in V with I is the highest, V_{upper} reaches the critical voltage V_c (= $E_c L$ μV) at the lowest I for a given $L_{p,smallest}$-value (namely for a given size of the largest crack), and, accordingly, the I_c-value corresponds to the lower bound, $I_{c,lower}$. In this way, case A gives the upper bound of voltage V_{upper}, lower bound of critical current, $I_{c,lower}$, and upper bound of n-value, n_{upper}, for the region.

Case B: another extreme case where the crack size of one section is far larger than that of the other sections. The voltage of the region is equal to the voltage of the section with the largest crack, since the voltages of the other sections are too low to contribute the region's voltage. This case gives the lower bound V_{lower} for the voltage of the region. As the increase in V with I is the lowest, V_{lower} reaches the V_c-value at the highest I, and the index n in the form of $V \propto I^n$ is the lowest for a given $L_{p,smallest}$ (namely for a given size of the largest crack). In this way, case B gives the lower bound of voltage V_{lower}, the upper bound of critical current, $I_{c,upper}$, and lower bound of n-value, n_{lower}, for the region.

The V_{upper}–I and V_{lower}–I curves of each region were calculated with eqs. (1), (2), (5) and (6) by finding the section with the largest crack, which has the smallest L_p-value, $L_{p,smallest}$, among the sections in each region. Then, from the calculated curves, the values of $I_{c,upper}$, $I_{c,lower}$, n_{upper} and n_{lower} were obtained and were compared with the simulation results of the I_c- and n-values.

Figure 3 shows the examples (Ex.(1), Ex.(2) and Ex.(3)) of (a, b, c) V–I curves of the 7.5 cm-region and the five 1.5 cm-sections in the region, and (a′, b′, c′) V–I, V_{upper}–I and V_{lower}–I curves of the 7.5 cm-region. (a, a′), (b, b′) and (c, c′) show the results of Ex.(1), Ex.(2) and Ex.(3), corresponding to small, intermediate and large difference in crack size among the five sections, respectively. In these examples, the ligament parameter of the smallest ligament (= largest crack)-section, $L_{p,smallest}$, was common ($L_{p,smallest} = 0.651$) while the ligament parameter values of other four sections were different among the examples.

In Fig. 3, while the V–I curve of the region exists in between the V_{upper}–I and V_{lower}–I curves in all examples, the V–I curve in Ex.(1) (small difference in crack size) is near to the V_{upper}–I curve, it shifts toward the V_{lower}–I curve with increasing difference in crack size (Ex.(2)) and approaches near to the V_{lower}–I curve at large difference in crack size (Ex.(3)). As the $L_{p,smallest}$-value is common in Ex.(1), Ex.(2) and Ex.(3), the V_{lower}–I and V_{upper}–I curves are common and hence the upper and lower bounds of I_c- and n-values are also common; $I_{c,upper} = 140$ A, $I_{c,lower} = 131$ A, $n_{upper} = 26.9$ and $n_{lower} = 12.1$. Concerning the influence of the largest crack-section and other sections on critical current and n-value of region, the following features are read from the results in Fig. 3.

(1) The largest crack in the region affects most significantly the V–I curve since the location of the V–I curve of the section with the largest crack is the nearest to the V–I curve of the region. On this point, the largest crack affects more significantly on both I_c- and n-values than the other size cracks.

(2) The difference in crack size among the sections also influences both on I_c- and n-values of the region, through the

change of the positional relation of the V–I curves among the sections, which change the V–I curve of the region. When the difference in crack size is small (Ex.(1) in Fig. 3 (a, a′)), the V–I curves of the sections exist near to each other. All sections contribute to synthesize the voltage of the region, and hence, the voltage V of the region rises sharply with increasing current I, resulting in lower I_c and higher n-value. On the other hand, when the difference in crack size is large (Ex.(3) in Fig. 3 (c, c′)), the V–I curves of the sections exist apart from each other. Thus, only one or a few sections contribute to synthesize the voltage of the region, and, hence, the voltage of the region increases gradually with current I, resulting in higher I_c and lower n-value under the given $L_{p,smallest}$-value (0.651). In this way, with increasing difference in crack size among sections, the I_c value obtained by simulation increases from 133 A in Ex.(1) to 136 A in Ex.2 and to 139 A in Ex.(3), but n-value decreases from 26.3 in Ex.(1) to 22.8 in Ex.(2) and to 17.1 in Ex.(3), as shown in Fig. 3.

(3) As the $L_{p,smallest}$-value is common (0.651) in Ex.(1), Ex.(2) and Ex.(3) in Fig. 3, the upper and lower bounds of I_c- and n-values for $L = 7.5$ cm are common in these examples; $I_{c,upper} = 140$ A, $I_{c,lower} = 131$ A, $n_{upper} = 26.9$ and $n_{lower} = 12.1$. The I_c- and n-values obtained by simulation for $L = 7.5$ cm ($I_c = 133$ A and $n = 26.3$ in Ex.(1), $I_c = 136$ A and $n = 22.8$ in Ex.(2), and $I_c = 139$ A and $n = 17.1$ in Ex.(3)) are in between the upper and lower bounds. This means that, while the upper and lower bounds of I_c- and n-values of region can be calculated by using the V–I curve of the smallest ligament (largest crack)-section, not only the size of the largest crack but also the difference in crack size among the sections affect the I_c- and n-values.

(4) The difference between the $I_{c,upper}$ and $I_{c,lower}$, normalized with respect to the critical current in the non-cracked state $I_{c0} = 200$ A, $(I_{c,upper} - I_{c,lower})/I_{c0}$, is $(140 - 131)/200 = 0.045$. The difference between n_{upper} and n_{lower}, normalized with respect to the n-value in the non-cracked state $n_0 = 40$, $(n_{upper} - n_{lower})/n_0$, is $(26.9 - 12.1)/40 = 0.37$ which is far higher than 0.045 for critical current. The difference in critical current between the upper and lower bounds, arising from the difference in crack size among the sections, was less than 10 A for $L = 7.5$ cm, which was less than 5% of the original critical current $I_{c0} = 200$ A. On the other hand, the difference in n-value between the upper and lower bounds was 37% of the original n-value $n_0 = 40$. It is suggested that the I_c is determined mainly by the size of the largest crack but n-value is determined by both of the size of the largest crack and the difference in crack size among the sections.

(5) The size of the largest crack is different among the regions between the voltage probes. The result stated in (4) suggests that, under the condition where the influence of the difference in crack size is small, the critical current distribution can be described from the viewpoint of the size distribution of the largest crack as a first approximation.

3.3 Relation of the ligament parameter of the smallest ligament (largest crack)-section in the region, $L_{p,smallest}$, to the critical current of the region, I_c

Figure 4 shows the plot of the I_c-values against the ligament parameter of the smallest ligament (largest crack)-section, $L_{p,smallest}$, for $L =$ (a) 1.5 cm, (b) 4.5 cm and (c) 7.5 cm, together with the calculated $I_{c,upper}$- and $I_{c,lower}$-values as a function of $L_{p,smallest}$. When the voltage probe spacing L is small, the difference between the $I_{c,upper}$ and $I_{c,lower}$ is small.

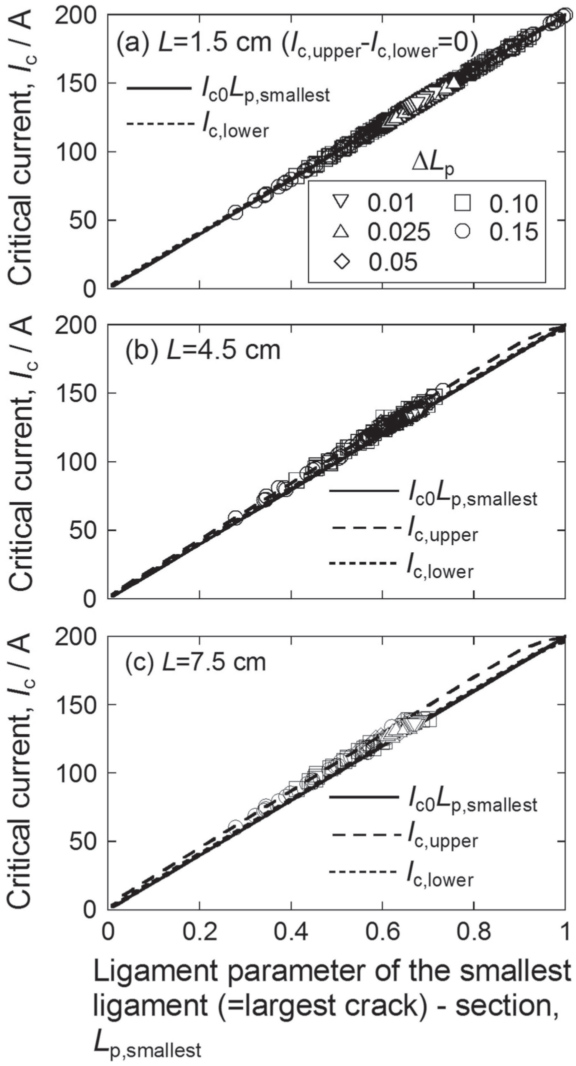

Fig. 4 Plot of the critical current (I_c) values obtained by simulation against the ligament parameter of the smallest ligament (largest crack)-section, $L_{p,smallest}$, for $L =$ (a) 1.5 cm, (b) 4.5 cm and (c) 7.5 cm, together with the calculated $I_{c0}L_{p,smallest}$-, $I_{c,upper}$- and $I_{c,lower}$-values as a function of $L_{p,smallest}$.

It is noted that the $I_{c,lower}$ value derived from case A for a given $L_{p,smallest}$-value is common for any L-value since case A corresponds to $\Delta L_p = 0$ (uniform crack size). It has been known experimentally that, when the voltage spacing is short such as 1.5 cm, shunting current at the cracked part is low and I_c is nearly given by $I_{c0}L_{p,smallest}$ in REBCO-coated tape.[2,4,6) Thus, under the condition of small L where $I_{c,upper}$–$I_{c,lower}$ is small, I_c is approximately given by[2,4,6)]

$$I_c \approx I_{c,lower} \approx I_{c0} L_{p,smallest} \tag{7}$$

The calculated $I_{c0}L_{p,smallest}$ as a function of $L_{p,smallest}$ is also presented with a solid line for each of $L = 1.5$ cm, 4.5 cm and 7.5 cm in Fig. 4. The $I_{c,lower}$ is almost the same as the $I_{c0}L_{p,smallest}$ for any $L_{p,smallest}$ value, showing that eq. (7) is hold for small L.

The average values of I_c, $I_{c,ave}$, for each value of ΔL_p (= 0.01, 0.025, 0.05, 0.1 and 0.15) and L (1.5 cm, 4.5 cm,

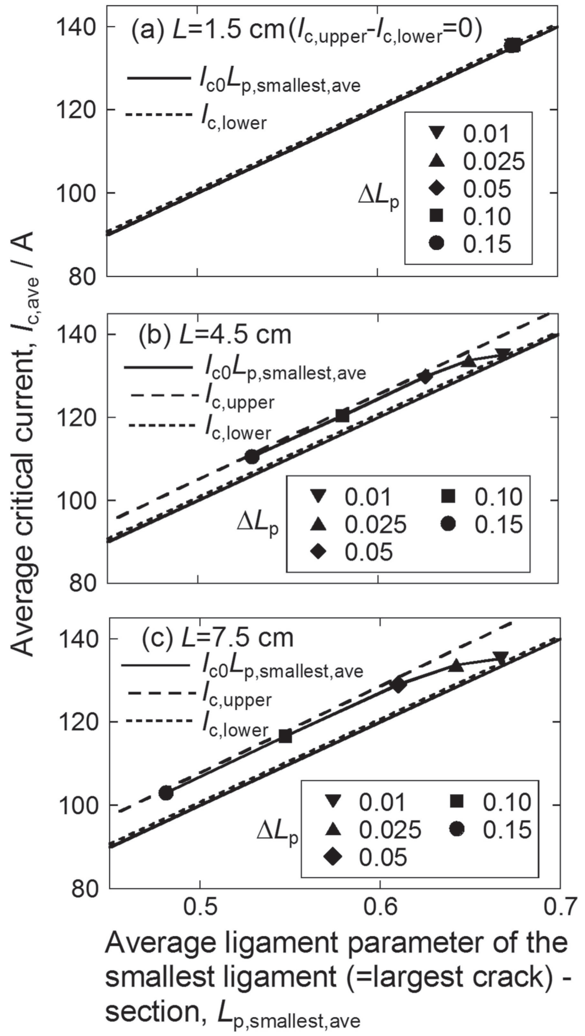

Fig. 5 Plot of the average critical current $I_{c,ave}$ obtained by simulation for $\Delta L_p = 0.01$, 0.025, 0.05, 0.1 and 0.15 against the average ligament parameter of the smallest ligament (largest crack)-section, $L_{p,smallest,ave}$. For comparison, the upper and lower bounds are drawn. (a), (b) and (c) show the result for $L = 1.5$ cm, 4.5 cm and 7.5 cm, respectively.

7.5 cm) were plotted against the average ligament parameter of the smallest ligament (largest crack)-section, $L_{p,smallest,ave}$, as shown in Fig. 5 (a, b, c). For comparison, the $I_{c,upper}$, $I_{c,lower}$ and $I_{c0}L_{p,smallest,ave}$ calculated as a function of $L_{p,smallest,ave}$ are superimposed in Fig. 5. The following features are read from Fig. 5.

The $I_{c,ave}$-value for $\Delta L_p = 0.01$ (very small distribution width of crack size) is very near to the lower bound since not only the section with the largest crack but also the other sections whose crack sizes are near to the size of the largest crack contribute to raise the voltage of the region. With increasing ΔL_p from 0.01, the V–I curves of the sections become apart from each other. As a result, the contribution of the second, third, ..., largest crack-sections to the voltage of the region becomes small as has been shown in Fig. 3. Thus the V of the region in relation to I becomes lower with increase in ΔL_p and it reaches V_c at higher I, resulting in higher I_c for a given size of the largest crack. In this way, while the I_c values are near to the lower bounds at small ΔL_p, they shift to the upper bounds with increasing ΔL_p.

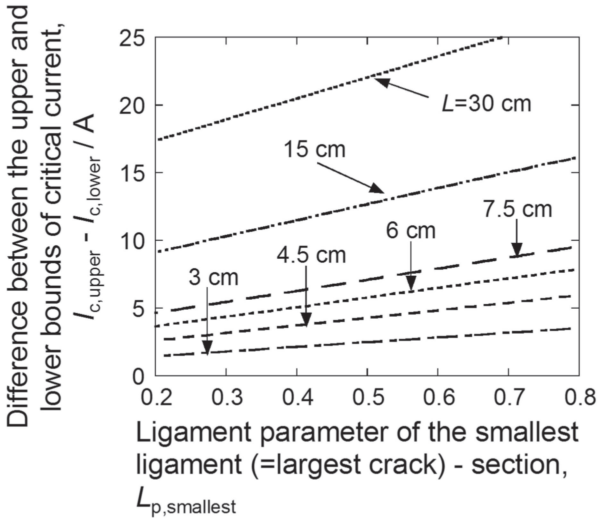

Fig. 6 Difference between the upper and lower bounds of critical current, $I_{c,upper}$–$I_{c,lower}$, as a function of the ligament parameter $L_{p,smallest}$ of the smallest ligament (largest crack)-section, for voltage probe spacing $L =$ 3~30 cm. The difference in critical current for a given size of the smallest ligament (size of the largest crack) arises due to the difference in the positional relation of the V–I curves of all sections (Fig. 3). In this figure, the statistically extreme cases A and B are taken up and the $I_{c,upper}$ and $I_{c,lower}$ are calculated from these extreme cases.

As shown in Figs. 4 and 5, the difference between the upper and lower bounds of the critical current, $I_{c,upper}$–$I_{c,lower}$, for a given smallest ligament parameter value, $L_{p,smallest}$, increases with increasing L. In order to examine the L-dependence of $I_{c,upper}$–$I_{c,lower}$ in detail, the $I_{c,upper}$–$I_{c,lower}$ values were calculated for wide range of $L_{p,smallest}$ and L. Figure 6 shows the calculated $I_{c,upper}$–$I_{c,lower}$ values as a function of $L_{p,smallest}$ for $L = 3\sim30$ cm. The result shows that, while the I_c is primarily determined by the size of the largest crack (Fig. 4), the I_c for a given size of the largest crack varies depending on the positional relation of the V–I curves among the sections, arising from the difference in crack size among the sections. The difference between the $I_{c,upper}$ and $I_{c,lower}$ is small when the voltage probe spacing L is small but it becomes large for large L. This, in turn, means that the I_c of short region is determined nearly by the size of largest crack, as has been shown in Fig. 4. Hence, the distribution of I_c of short region can be described by the distribution of the size of the largest crack as a first approximation.

3.4 Statistical analysis of the distribution of I_c-values in relation to the distribution of the size of the largest crack monitored by the distribution of the smallest ligament parameter $L_{p,smallest}$

As shown in subsections 3.2 and 3.3, the I_c is determined not only by the $L_{p,smallest}$ but also by the positional relation of the V–I curves among the sections in the region. The latter effect, reflecting the difference in crack size among the sections, is rather small within the small voltage probe spacing ($L \leq 7.5$ cm in this work). Under this condition, the critical current is approximately given by $I_c = I_{c0}L_{p,smallest}$ (eq. (7)) as known from the plot of I_c values against the corresponding $L_{p,smallest}$ values in Fig. 4. Thus, when the distribution of $L_{p,smallest}$ is known, the distribution of critical current can be predicted as a first approximation. In this

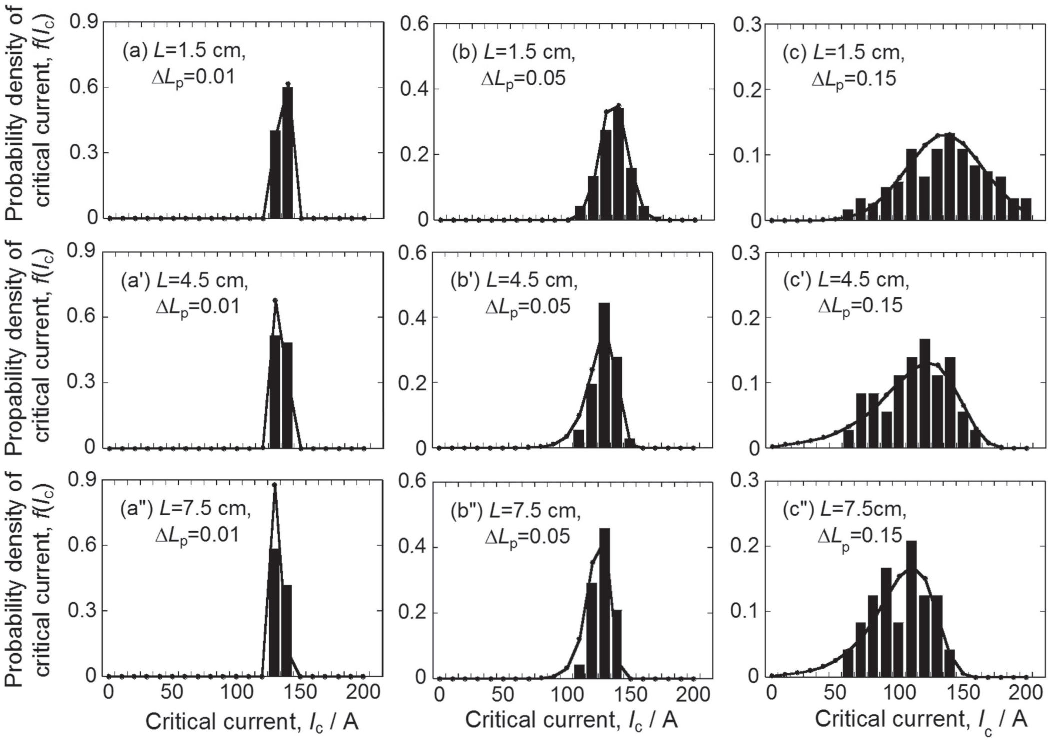

Fig. 7 Distribution histograms of critical current (I_c) values obtained by simulation under the condition of $\Delta L_p = 0.01$ (a, a′, a″), 0.05 (b, b′, b″) and 0.15 (c, c′, c″) for $L = 1.5$ cm (a, a′, a″), 4.5 cm (b, b′, b″) and 7.5 cm (c, c′, c″) in comparison with the distribution curves calculated in a step of 10 A critical current in the range of 0 A to 200 A.

subsection, it is attempted to describe the distribution of I_c under small L by using eq. (7) through the derivation of the distribution of $L_{p,smallest}$ values.

In the present work, the distribution of the ligament parameter L_p was given by the normal distribution (eqs. (3) and (4)). We use this distribution function for L_p and the extreme value distribution of Gumbel[25] for the smallest value of L_p, $L_{p,smallest}$, among the N sections ($N = 3$ and 5 for $L = 4.5$ and 7.5 cm, respectively). The $L_{p,smallest}$ refers to the section with the smallest ligament; namely the section with the largest crack among N sections. The cumulative distribution function $\Phi(L_{p,smallest})$ of the smallest value of L_p, $L_{p,smallest}$, based on the Gumbel's distribution function for the extreme values, is expressed as[25]

$$\Phi(L_{p,\,smallest}) = 1 - \exp\left\{-\exp\left(\frac{L_{p,\,smallest} - \lambda}{\alpha}\right)\right\} \quad (8)$$

Since the normal distribution was used as the distribution function of the L_p value, the positional parameter λ and the scale parameter α in eq. (8) were obtained by using the cumulative distribution function $F(L_p)$ (eq. (3)) and the probability density function $f(L_p)$ (eq. (4)) as the values satisfying the following formulations,[25]

$$F(\lambda) = 1/N \quad (9)$$

$$\alpha = 1/\{Nf(\lambda)\} \quad (10)$$

Substituting the values of λ and α obtained by eqs. (9) and (10) into eq. (8), we can calculate the distribution of $L_{p,smallest}$. Combining the obtained distribution of $L_{p,smallest}$ with eq. (7) ($I_c \approx I_{c0}L_{p,smallest}$) which is an approximate expression of the relationship between $I_{c,lower}$ and $L_{p,smallest}$ (Figs. 4 and 5), we have the cumulative distribution function of I_c, $\Omega(I_c)$, in the form,

$$\Omega(I_c) = 1 - \exp\left\{-\exp\left(\frac{I_c/I_{c0} - \lambda}{\alpha}\right)\right\} \quad (11)$$

Figure 7 shows the distributions of the I_c values obtained by simulation under the condition of $\Delta L_p = 0.01$ (a, a′, a″), 0.05 (b, b′, b″) and 0.15 (c, c′, c″) for $L = 1.5$ cm (a, b, c), 4.5 cm (a′, b′, c′) and 7.5 cm (a″, b″, c″) in comparison with the distribution calculated by eq. (11) in step of 10 A critical current in the range of 0 to 200 A. The calculation result almost describes the simulation result. In this way, it was shown that, when the voltage probe spacing is small (when the specimen is short), the distribution of I_c can be described as a first approximation from the distribution of crack size.

4. Conclusions

(1) The experimentally observed feature that I_c decreases with increase in distribution width of crack size and with increase in voltage probe spacing was reproduced by the present simulation.
(2) The largest crack among all cracks in the region between the voltage probes plays a dominant role in determination of critical current under small voltage probe spacing.
(3) Under a given size of the smallest ligament (= under a given size of the largest crack), the large difference in crack size among the sections acts to raise critical current value and to reduce n-value. The extent of the reduction of n-value with increasing difference in crack

size among the sections is higher than that of the increase of critical current.

(4) Under the small voltage probe spacing, the distribution of critical current and its dependence on voltage probe spacing and distribution width of crack size were described as a first approximation, using the Gumbel's extreme value distribution.

REFERENCES

1) D.C. van der Laan, J.W. Ekin, F.F. Douglas, C.C. Clickner, T.C. Stauffer and L.F. Goodrich: Supercond. Sci. Technol. **23** (2010) 072001.
2) S. Ochiai, T. Arai, A. Toda, H. Okuda, M. Sugano, K. Osamura and W. Prusseit: J. Appl. Phys. **108** (2010) 063905.
3) H.-S. Shin, J. Marlon, H. Dedicatoria, H.-S. Kim, N.-J. Lee, H.-S. Ha and S.-S. Oh: IEEE Trans. Appl. Supercond. **21** (2011) 2997–3000.
4) S. Ochiai, H. Okuda, T. Arai, S. Nagano, M. Sugano and W. Prusseit: Cryogenics **51** (2011) 584–590.
5) S. Ochiai, T. Arai, S. Nagano, H. Okuda, M. Sugano, K. Osamura and W. Prusseit: J. Japan Inst. Copper **51** (2012) 217–222.
6) S. Ochiai, H. Okuda, T. Arai, M. Sugano, K. Osamura and W. Prusseit: Mater. Trans. **54** (2013) 269–275.
7) H. Oguro, T. Suwa, T. Suzuki, S. Awaji, K. Watanabe, M. Sugano, S. Machiya, M. Sato, T. Koganezawa, T. Machi, M. Yoshizumi and T. Izumi: IEEE Trans. Appl. Supercond. **23** (2013) 8400304.
8) S. Ochiai, H. Okuda, M. Sugano, S.-S. Oh and H.-S. Ha: Mater. Trans. **56** (2015) 1558–1564.
9) Y. Fang, S. Danyluk and M.T. Lanagan: Cryogenics **36** (1996) 957–962.
10) S. Ochiai, D. Doko, H. Okuda, S.S. Oh and D.W. Ha: Supercond. Sci. Technol. **19** (2006) 1097–1103.
11) S. Ochiai, M. Fujimoto, H. Okuda, S.S. Oh and D.W. Ha: J. Appl. Phys. **105** (2009) 063912.
12) J.K. Shin, S. Ochiai, H. Okuda, M. Sugano and S.-S. Oh: Supercond. Sci. Technol. **21** (2008) 115007.
13) S. Ochiai, M. Fujimoto, J.K. Shin, H. Okuda, S.S. Oh and D.W. Ha: J. Appl. Phys. **106** (2009) 103916.
14) S. Ochiai, H. Okuda, H. Matsubayashi, K. Osamura and A. Otto: Mater. Trans. **57** (2016) 709–715.
15) H. Kitaguchi, A. Matsumoto, H. Hatakeyama and H. Kumakura: Physica C **401** (2004) 246–250.
16) Y. Miyoshi, E.P.A. Van Lanen, M.M. Dhallé and N. Nijhuits: Supercond. Sci. Technol. **22** (2009) 085009.
17) N. Banno, D. Uglietti, B. Seeber, T. Takeuchi and R. Flükiger: Supercond. Sci. Technol. **18** (2005) 284–288.
18) J.J. Gannon, Jr., A.P. Malozemoff, R.C. Diehl, P. Antaya and A. Mori: IEEE Trans. Appl. Supercond. **23** (2013) 8002005.
19) T. Nakamura, Y. Takamura, N. Amemiya, K. Nakao and T. Izumi: Cryogenics **63** (2014) 17–24.
20) S. Ochiai, H. Okuda and N. Fujii: Mater. Trans. **58** (2017) 679–687.
21) S. Ochiai, H. Okuda and N. Fujii: Mater. Trans. **58** (2017) 1469–1478.
22) S. Ochiai, H. Okuda and N. Fujii: Mater. Trans. **59** (2018) 1380–1388.
23) S. Ochiai, H. Okuda and N. Fujii: Mater. Trans. **59** (2018) 1628–1636.
24) S. Ochiai, H. Okuda and N. Fujii: Mater. Trans. **60** (2019) 574–582.
25) E.J. Gumbel: *Statistics of Extremes*, (Columbia Univ. Press, New York, 1958) pp. 156–254.